Molecular orientation studies by pulsed electron-electron double resonance experiments

A. Marko, D. Margraf, H. Yu, Y. Mu, G. Stock, and T. Prisner

Citation: The Journal of Chemical Physics **130**, 064102 (2009); doi: 10.1063/1.3073040
View online: http://dx.doi.org/10.1063/1.3073040
View Table of Contents: http://scitation.aip.org/content/aip/journal/jcp/130/6?ver=pdfcov
Published by the AIP Publishing

Molecular orientation studies by pulsed electron-electron double resonance experiments

A. Marko,[1,a)] D. Margraf,[1] H. Yu,[2] Y. Mu,[2] G. Stock,[1] and T. Prisner[1]
[1]*Institute of Physical and Theoretical Chemistry, J. W. Goethe University, Max-von-Laue-Str. 7, D-60438 Frankfurt, Germany*
[2]*School of Biological Sciences, Nanyang Technological University, Singapore 637551, Singapore*

(Received 8 November 2008; accepted 29 December 2008; published online 9 February 2009)

Pulsed electron-electron double resonance (PELDOR) has proven to be a valuable tool to measure the distribution of long range distances in noncrystalline macromolecules. These experiments commonly use nitroxide spin labels as paramagnetic markers that are covalently attached to the macromolecule at specific positions. Unless these spin labels are flexible in such a manner that they exhibit an almost random orientation, the PELDOR signals will—apart from the interspin distance—also depend on the orientation of the spin labels. This effect needs to be considered in the analysis of PELDOR signals and can, moreover, be used to obtain additional information on the structure of the molecule under investigation. In this work, we demonstrate that the PELDOR signal can be represented as a convolution of a kernel function containing the distance distribution function and an orientation intensity function. The following strategy is proposed to obtain both functions from the experimental data. In a first step, the distance distribution function is estimated by the Tikhonov regularization, using the average over all PELDOR time traces with different frequency offsets and neglecting angular correlations of the spin labels. Second, the convolution relation is employed to determine the orientation intensity function, using again the Tikhonov regularization. Adopting small nitroxide biradical molecules as simple examples, it is shown that the approach works well and is internally consistent. Furthermore, independent molecular dynamics simulations are performed and used to calculate PELDOR signals, distance distributions, and orientational intensity functions. The calculated and experimental results are found to be in excellent overall agreement. © *2009 American Institute of Physics*. [DOI: 10.1063/1.3073040]

I. INTRODUCTION

Pulsed electron-electron double resonance[1–7] (PELDOR) is a well-established method to determine long range distances and distance distributions in noncrystalline macromolecular systems. Similar to fluorescence resonance energy transfer[8] which invokes the electric dipole-dipole interaction, this technique uses the magnetic dipole-dipole interaction between two paramagnetic centers in order to measure distances in the range of 2–8 nm. The magnetic interaction depends on the *g*-tensor of both paramagnetic centers or molecules, the distance $r=|\boldsymbol{r}|$ between the two unpaired electron spins, and on the angle Θ between the vector $\boldsymbol{r}$ and the external magnetic field $\boldsymbol{B}_0$.

In biological systems such as proteins, DNA, or RNA, nitroxide spin labels are commonly employed as paramagnetic markers which are covalently attached to the macromolecule at specific positions via site-directed mutagenesis or chemical synthesis.[9–15] Usually these spin labels are flexible and therefore exhibit an almost random orientation with respect to their interconnecting dipolar vector $\boldsymbol{r}$. In such cases, the only free parameter determining the PELDOR time-domain signals is the distribution $f(r)$ of the distance between the two unpaired electron spins. The function $f(r)$ can be extracted from PELDOR time traces, e.g., via the Tikhonov regularization,[16–20] thus allowing a quantitative and parameter-free determination of long range distances in macromolecular systems. Additionally, the shape of the distance distribution function $f(r)$ contains information regarding the conformational flexibility of the molecular system.

The situation differs for rigid spin labels and covalently bound native paramagnetic cofactors in proteins. Their mutual orientation as well as their orientations with respect to the dipolar vector $\boldsymbol{r}$ are often constrained by covalent or hydrogen bonds. At high magnetic field strengths, the anisotropy of the *g*-tensor of such organic systems can be spectrally resolved. This allows us to perform PELDOR experiments where only paramagnetic molecules with a specific orientation of $\boldsymbol{r}$ with respect to the external magnetic field $\boldsymbol{B}_0$ are pumped and probed. Under such conditions, the dipolar angle Θ determines not only the dipolar splitting but also the contributions of different orientations to the total PELDOR signal. These contributions can be described by the orientation intensity function $\lambda(\cos\Theta)$. Apart from Θ, the function $\lambda(\cos\Theta)$ also depends on the properties of the microwave pump and probe pulses (e.g., frequencies and field strengths) and on the geometry of the paramagnetic centers. Note that $\lambda(\cos\Theta)$ is constant in the absence of correlation between orientations of the paramagnetic centers. Hence, PELDOR measurements with variable pump and probe frequencies give rise to assigning not only the distance but also

[a)]Electronic mail: marko@prisner.de.

the mutual orientation of two paramagnetic centers. Employing high magnetic fields, this was recently demonstrated for a dimer of ribonucleotide reductase with tyrosyl radicals as native paramagnetic centers.[21,22]

Recently, it has been reported that partial orientation correlations might also exist between nitroxides.[6] This effect can be caused by sterical restrictions within the macromolecule or by hydrophobic interactions between the spin label and the biomolecule. If such correlations exist, they need to be explicitly taken into account in order to obtain quantitative structural constraints and dynamical properties of the macromolecule. Fortunately, the mutual orientation of nitroxides can be easily proven experimentally via a systematic variation of the probe frequency within the spectral range of the nitroxide. Depending on the magnetic field strength, either the anisotropic nitrogen hyperfine interaction tensor or the anisotropic g-tensor can be used to achieve orientation selectivity of the probe pulses.[23–26] Adopting small organic binitroxide model systems, it was recently demonstrated that X-band PELDOR time traces can be employed to deduce the conformational flexibility of the molecule.[26] In this case, the conformational flexibility could be satisfactory described by a simple geometrical model. A more complex situation arises in biological macromolecules, where the restricted flexibility of the spin label and the biomolecule itself are unknown. This case requires a method capable disentangling the distance information $f(r)$ from the orientational information $\lambda(\cos\Theta)$.

In this work, we show that a PELDOR signal can be represented as a convolution of the orientation intensity function $\lambda(\cos\Theta)$ and a kernel function containing the distance distribution function $f(r)$. We use this relation to determine both $f(r)$ and $\lambda(\cos\Theta)$ from experimental data. The following strategy is employed. In a first step, the distance distribution $f(r)$ is estimated by the Tikhonov regularization,[16] using the average of all PELDOR time traces with different probe frequency offsets and neglecting angular correlations of the spin labels. Second, the convolution relation is employed to determine the orientation intensity function $\lambda(\cos\Theta)$ via the Tikhonov regularization of the experimental data. To study its potential and numerical stability, the method is first validated by considering various computer-generated PELDOR time traces with given functions $\lambda(\cos\Theta)$. Then the approach is applied to analyze PELDOR experiments on two nitroxide biradicals. The obtained experimental results for the functions $f(r)$ and $\lambda(\cos\Theta)$ are compared to results obtained by independent all-atom molecular dynamics simulations in explicit solvent. We obtain an excellent overall agreement between theory and experiment, suggesting the applicability of the proposed approach.

II. THEORY

A. Calculation of PELDOR signals

To describe the PELDOR experiments, it is helpful to first introduce an appropriate coordinate system as shown in Fig. 1(a). We consider a molecule containing two nitroxide radicals, whose unpaired electrons are connected by the vector $\boldsymbol{r}$. Each nitroxide radical is associated with its principal coordinate system with unit vectors $\{\boldsymbol{x}_1,\boldsymbol{y}_1,\boldsymbol{z}_1\}$ and $\{\boldsymbol{x}_2,\boldsymbol{y}_2,\boldsymbol{z}_2\}$, whose x-axis is parallel to the NO bond and whose z-axis coincides with the plane normal of the radical (see Fig. 1). The orientation of the two radicals is characterized by the Euler angles $(\alpha_1,\beta_1,\gamma_1)\equiv\boldsymbol{o}_1$ and $(\alpha_2,\beta_2,\gamma_2)\equiv\boldsymbol{o}_2$. Furthermore, we introduce the dipolar coordinate system with unit vectors $\{\boldsymbol{x},\boldsymbol{y},\boldsymbol{z}\}$, whose z-axis coincides with the interspin vector $\boldsymbol{r}$. The orientation of the external magnetic field $\boldsymbol{B}_0$ in this coordinate system is given by the polar angle Θ and the azimuth angle Φ.

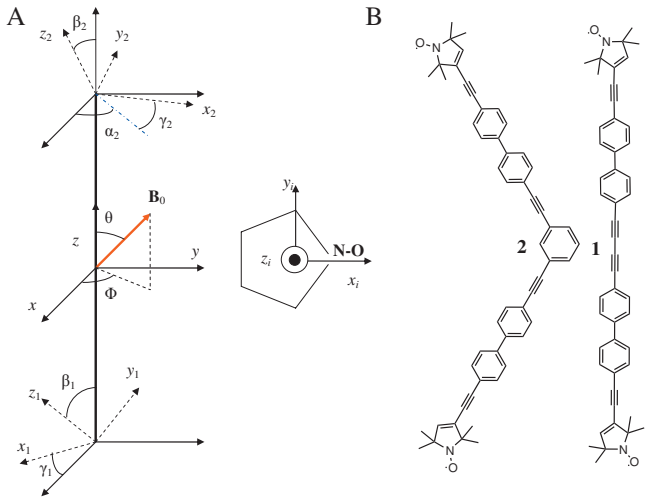

FIG. 1. (Color) (a) Three coordinate systems are used to describe the PELDOR experiments: The dipolar coordinate system $\{\boldsymbol{x},\boldsymbol{y},\boldsymbol{z}\}$ whose z-axis coincides with the interspin vector $\boldsymbol{r}$, and the principal coordinate systems $\{\boldsymbol{x}_1,\boldsymbol{y}_1,\boldsymbol{z}_1\}$ and $\{\boldsymbol{x}_2,\boldsymbol{y}_2,\boldsymbol{z}_2\}$ of the first and second nitroxide radicals, respectively. The orientation of the two radicals is described by the Euler angles $(\alpha_1,\beta_1,\gamma_1)\equiv\boldsymbol{o}_1$ and $(\alpha_2,\beta_2,\gamma_2)\equiv\boldsymbol{o}_2$. Angles Θ and Φ define the direction of the magnetic field $\boldsymbol{B}_0$. (b) Structures of the studied model compounds: (1) linear nitroxide biradical and (2) bent nitroxide biradical.

Having defined the relative orientations of the nitroxides and of the external field, we are able to calculate the resonance frequency ω_r of the two electron spins. It is determined by (i) the Zeeman interaction with the external magnetic field, (ii) the hyperfine interaction with the ^{14}N nucleus, and (iii) local field fluctuations leading to inhomogeneous line broadening δb. This yields[5,24,25]

$$\omega_r(\Theta,\Phi,\boldsymbol{o},m) = \gamma_0[B_0 g_{\mathrm{eff}}(\Theta,\Phi,\boldsymbol{o})/g_e + mA_{\mathrm{eff}}(\Theta,\Phi,\boldsymbol{o}) + \delta b], \tag{1}$$

where $\boldsymbol{o}=\boldsymbol{o}_1,\boldsymbol{o}_2$ represents the Euler angles of spin 1 and 2, respectively, γ_0 denotes the gyromagnetic ratio of electron, g_e is the g-value of the free electron, and the quantum number $m=-1,0,1$ accounts for the state of the nuclear spin. Functions $g_{\mathrm{eff}}(\Theta,\Phi,\boldsymbol{o})$ and $A_{\mathrm{eff}}(\Theta,\Phi,\boldsymbol{o})$ are effective values of the g-tensor and hyperfine interaction tensor A in the di-

polar coordinate system, respectively. They can be calculated from[5]

$$T_{\mathrm{eff}}^2(\Theta,\Phi,\boldsymbol{o}) = T_{xx}^2 + (T_{yy}^2 - T_{xx}^2)[\sin\Theta\sin\gamma\cos(\alpha-\Phi) + \sin\Theta\cos\gamma\sin(\alpha-\Phi)\cos\beta + \cos\Theta\cos\gamma\sin\beta]^2 + (T_{zz}^2 - T_{xx}^2) \times[\sin\Theta\sin\beta\sin(\alpha-\Phi) + \cos\Theta\cos\beta]^2, \quad (2)$$

where T can be either the g-tensor or the A-tensor. The function T_{eff} is symmetrical with respect to the origin of the coordinate system, i.e., $T_{\mathrm{eff}}(\Theta,\Phi,\boldsymbol{o}) = T_{\mathrm{eff}}(\pi-\Theta,\pi+\Phi,\boldsymbol{o})$. For $\boldsymbol{o}=0$, Eq. (2) simplifies to $T_{\mathrm{eff}}^2(\Theta,\Phi,0) = T_{xx}^2\sin^2\Theta\cos^2\Phi + T_{yy}^2\sin^2\Theta\sin^2\Phi + T_{zz}^2\cos^2\Theta$.

We are concerned with a dead-time free PELDOR experiment,[27] in which four microwave pulses are applied. In order to excite the largest possible amount of spins, the frequency of the pump pulse is tuned to the center of the nitroxide spectrum. The frequency of the three probe pulses is chosen to be larger than the pump-pulse frequency by an offset $\Delta\nu$. It excites electron spin transitions with nitrogen nuclear spin state $m=+1$. If one of the radicals is excited by the probe pulses (the A-spin) and the other one by the pump pulse (the B-spin), the intensity of the refocused Hahn echo which is formed by the probe pulses will be modulated depending on the delay time T between probe and pump pulses. For a given probe frequency ν, the PELDOR signal $v(T,\nu)$ can be written as[26,28]

$$v(T,\nu) = v_0(\nu) + \int_0^{\pi/2} d\Theta\,\sin\Theta u(\nu,\Theta,\boldsymbol{o}_1,\boldsymbol{o}_2) \times\left[\cos\left(D\frac{1-3\cos^2\Theta}{r^3}T\right) - 1\right]. \quad (3)$$

Here $D=\mu_0(g_e\mu_B)^2/(4\pi\hbar)=2\pi\times 52.04$ MHz nm^3 is the dipolar interaction constant, which is expressed for a weakly anisotropic g-tensor through the following fundamental physical constants: the magnetic susceptibility of vacuum, μ_0, the g-value of free electron, g_e, the Bohr magneton, μ_B, and Planck's constant h. $v_0(\nu)$ is the refocused Hahn-echo signal formed by the three probe pulses with frequency ν in the absence of the pump pulse.

The central quantity entering the calculation of the PELDOR signal is the function $u(\nu,\Theta,\boldsymbol{o}_1,\boldsymbol{o}_2)$. It describes the signal intensity modulation, which is proportional to the magnetization of the A spin and in addition to the flip probability of the B spin. A general strategy to derive $u(\nu,\Theta,\boldsymbol{o}_1,\boldsymbol{o}_2)$ was described in Refs. 24 and 25. Here, we only present a brief derivation of $u(\nu,\Theta,\boldsymbol{o}_1,\boldsymbol{o}_2)$ in order to establish our notation and pulse sequence. We first introduce the electron spin Rabi frequency Ω_i, which is caused by microwave excitation with frequency ω_i and field strength B_{1i}, i.e.,

$$\Omega_i^2 = \gamma_0^2 B_{1i}^2 + (\omega_i - \omega_r)^2, \quad (4)$$

where $i=A,B$ indicates the probe and pump pulses, respectively. In our experiments we applied three probe pulses with the same duration t_A, but the last two π-pulses had double field strength, i.e., $B'_{1A}=2B_{1A}$. The corresponding Rabi frequency Ω'_A is found according to Eq. (4) with B'_{1A} instead of B_{1A}. After the application of three detection pulses, the x-component of the spin echo magnetization is equal to[24,25,29]

$$m_x(\omega_A,\Theta,\Phi,\boldsymbol{o},m,\delta b) = \frac{\gamma_0 B_{1A}}{\Omega_A}\sin(\Omega_A t_A)\frac{\gamma_0^4 B_{1A}'^4}{4\Omega_A'^4} \times[1-\cos(\Omega'_A t_A)]^2. \quad (5)$$

This quantity depends via the Rabi frequency Ω [Eq. (4)] on the probe pulse carrier frequency ω_A and via the resonance frequency ω_r [Eq. (1)] on the magnetic field orientation Θ, Φ, the radical orientation $\boldsymbol{o}$, the nuclear spin state m, and the field fluctuation δb.

To calculate the total transversal magnetization, the magnetization m_x of the A spin is weighted by the flip probability of the B spin. This probability is given by[24,25,29]

$$p(\Theta,\Phi,\boldsymbol{o},m,\delta b) = \frac{\gamma_0^2 B_{1B}^2}{2\Omega_B^2}[1-\cos(\Omega_B t_B)], \quad (6)$$

for the pump pulse of a length t_B. Hence, the total transversal magnetization for both unpaired spins can be written as

$$\xi(\omega_A,\Theta,\Phi,\boldsymbol{o}_1,\boldsymbol{o}_2,m_1,m_2,\delta b_1,\delta b_2) = m_x(\omega_A,\Theta,\Phi,\boldsymbol{o}_1,m_1,\delta b_1)p(\Theta,\Phi,\boldsymbol{o}_2,m_2,\delta b_2) + m_x(\omega_A,\Theta,\Phi,\boldsymbol{o}_2,m_2,\delta b_2)p(\Theta,\Phi,\boldsymbol{o}_1,m_1,\delta b_1). \quad (7)$$

The experimentally measured magnetization is given as an average (i) over all ^{14}N nuclear spin states m_1 and m_2, (ii) over the azimuthal angle Φ, and (iii) over the inhomogeneous line shape broadening δb (which is assumed to be Gaussian). This leads to the desired expression for the signal intensity function

$$u(\nu,\Theta,\boldsymbol{o}_1,\boldsymbol{o}_2) = \sum_{m_1,m_2}\langle\xi(\omega_A,\Theta,\Phi,\boldsymbol{o}_1,\boldsymbol{o}_2,m_1,m_2,\delta b_1,\delta b_2)\rangle_{\Phi,\delta b_1,\delta b_2}. \quad (8)$$

A similar expression can be derived for the refocused Hahn echo magnetization $v_0(\nu)$ in the absence of the pump pulse.

Equation (3) describes the PELDOR signal by assuming a single conformation of the molecule. In liquid solution, however, the molecule undergoes thermal fluctuations, resulting in an ensemble of $i=1,\ldots,N$ molecular structures with various dipolar distances r_i and spin label orientations $\boldsymbol{o}^{(i)}$. Assuming that this thermal distribution of conformational states is preserved in a PELDOR experiment using a frozen sample,[26] the total PELDOR signal $V(T,\nu)$ is given as an average over this distribution

$$V(T,\nu) = V_0(\nu) + \sum_{i=1}^{N}\int_0^{\pi/2} d\Theta\,\sin\Theta u(\nu,\Theta,\boldsymbol{o}_1^{(i)},\boldsymbol{o}_2^{(i)}) \times\left[\cos\left(D\frac{1-3\cos^2\Theta}{r_i^3}T\right) - 1\right], \quad (9)$$

where N is the total number of biradicals and $V_0(\nu) = Nv_0(\nu)$. This expression together with Eqs. (4)–(8) represent an in principle straightforward prescription to calculate

the measured PELDOR signal, in case the experimental conditions (e.g., T, ν, B_{1A}, and B_{1B}) and the ensemble of molecular structures (determining, e.g., Θ, $\boldsymbol{o}_1^{(i)}$, and $\boldsymbol{o}_2^{(i)}$) are given. As demonstrated in Sec. IV, the latter information can be obtained from molecular dynamic simulations, which together with Eq. (9) provide a *first principles* approach to model PELDOR experiments.

B. Determination of the orientation intensity function

As shown above, the measured PELDOR signal depends in a complicated way on both experimental conditions and on the structure of the molecular system. In an experimental study, however, one is typically interested to solve the inverse problem. That is, given some experimental data $V(T,\nu)$, one wants to determine the underlying molecular structure causing the signal. From Eq. (9) it is obvious that such an inversion needs to invoke several assumptions. The central approximation we are going to make is to assume that the conformational average $\langle\ldots\rangle=\frac{1}{N}\Sigma_{i=1}^{N}(\ldots)$ in Eq. (9) can be approximated by the product of two averages, i.e.,

$$\left\langle u(\nu,\Theta,\boldsymbol{o}_1^{(i)},\boldsymbol{o}_2^{(i)})\cos\left(D\frac{1-3\cos^2\Theta}{r_i^3}T\right)\right\rangle = \langle u(\nu,\Theta,\boldsymbol{o}_1^{(i)},\boldsymbol{o}_2^{(i)})\rangle\left\langle\cos\left(D\frac{1-3\cos^2\Theta}{r_i^3}T\right)\right\rangle. \quad (10)$$

This factorization is justified, if the fluctuations of the spin label distances r are only weakly correlated with the fluctuations of the orientation $\boldsymbol{o}_1$, and $\boldsymbol{o}_2$. By calculating PELDOR signals with and without approximation (10), it was found for both considered molecules (see Fig. 1) that the difference between the two results is much smaller than the noise level of the experimental data. Considering biomolecules which are much larger and much more flexible than the small organic molecules adopted here, factorization (10) should be virtually exact.

Introducing $z=\cos\Theta$, the above factorization allows us to write the normalized PELDOR signal $S(T,\nu)=V(T,\nu)/V_0(\nu)$ in the form of a Fredholm integral equation of the first kind[19]

$$S(T,\nu)=1+\int_0^1\lambda(z,\nu)K(z,T)dz, \quad (11)$$

with the kernel function

$$K(z,T)=\frac{1}{N}\sum_i^N\left[\cos\left(D\frac{1-3z^2}{r_i^3}T\right)-1\right], \quad (12)$$

and the orientation intensity function

$$\lambda(z,\nu)=\frac{1}{V_0(\nu)}\sum_i^N u(\nu,\Theta,\boldsymbol{o}_1^{(i)},\boldsymbol{o}_2^{(i)}). \quad (13)$$

Equations (11)–(13) represent the central theoretical result of this paper. Representing the PELDOR signal as a convolution of two functions, $K(z,T)$ and $\lambda(z,\nu)$, the formulation allows us to calculate one of the functions provided if the other is known. For example, by assuming that the distances between the radical electrons are described by a Gaussian distribution $f(r,r_0,\sigma)=(2\pi\sigma^2)^{-1/2}\exp[-(r-r_0)^2/(2\sigma^2)]$, the resulting kernel is

$$K(z,T)=\frac{1}{\sqrt{2\pi\sigma^2}}\int_0^\infty\exp\left[-\frac{(r-r_0)^2}{2\sigma^2}\right]\times\left[\cos\left(D\frac{1-3z^2}{r^3}T\right)-1\right]dr. \quad (14)$$

In a second step, this result in combination with Eq. (11) can be employed to calculate the orientation intensity function $\lambda(z,\nu)$ from the experimental data.

We note that the function $\lambda(z,\nu)$ has two important features. First, if it is constant orientation selection will not occurs in the system. Second, at long times, when all PELDOR oscillations are damped, the asymptotic value of the signal is given by

$$S(T\to\infty,\nu)=1-\int_0^1\lambda(z,\nu)dz. \quad (15)$$

Assuming that an explicit form of the kernel is given, Eq. (11) can be solved numerically to deduce the intensity function $\lambda(z,\nu)$. To this end, we discretize the time T into L steps of length $\Delta T=T_{\max}/L$ and the parameter $z\in[0,1]$ into M steps of length $\Delta z=1/M$. This allows us to represent Eq. (11) in matrix form as

$$s_i=\sum_j K_{ij}\lambda_j \quad \text{or} \quad \boldsymbol{s}=\hat{K}\boldsymbol{\lambda}, \quad (16)$$

where $s_i\equiv S(T_i,\nu)-1$, $K_{ij}\equiv K(T_i,z_j)\Delta z$, and $\lambda_j=\lambda(z_j,\nu)$. Expression (16) constitutes an overdetermined system of linear equations, i.e., it represents an ill-posed problem whose solutions may be unstable. As a consequence, small differences in the experimental data, such as noise, can lead to large deviations of the estimated results for λ. To solve Eq. (16), we utilize Tikhonov regularization[16–20] in order to minimize the functional

$$\|\boldsymbol{s}_{\exp}-\hat{K}\boldsymbol{\lambda}\|+\alpha\left\|\frac{d^2\lambda(z)}{dz^2}\right\|\to\min. \quad (17)$$

Here, α is a regularization parameter that depends on the quality of the experimental data and determines the smoothness of the solution. The above expression is minimized, when

$$\boldsymbol{\lambda}=|\hat{K}^T\hat{K}+\alpha\hat{D}^T\hat{D}|^{-1}\hat{K}^T\boldsymbol{s}_{\exp}, \quad (18)$$

where $\hat{D}$ is the second derivative operator written in matrix representation.

To study its performance and numerical stability, the method was first validated by considering various computer-generated PELDOR time traces with polynomial test functions $\lambda_i(z)$, see Fig. 2. We assumed kernel function (14) with Gaussian parameters $r_0=3$ nm and $\sigma=0.1$ nm, and added Gaussian noise of zero mean and 0.75% of the total echo amplitude to the PELDOR signals. The resulting set of signals was employed to find the function $\lambda(z)$ on the basis of the Tikhonov regularization method, assuming a regularization parameter of $\alpha=50$. Figure 2 demonstrates that the regularized orientation intensity functions are in good agreement

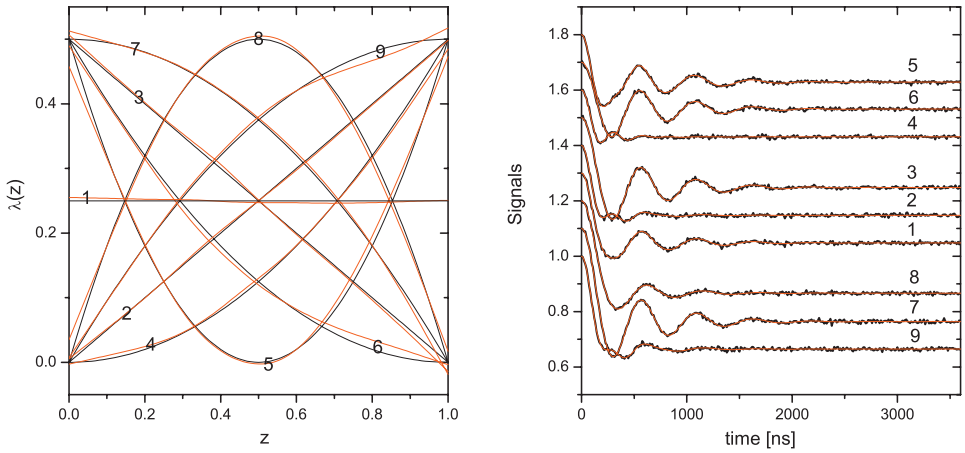

FIG. 2. (Color) Validation of the proposed deconvolution method of synthesized PELDOR signals, assuming a Gaussian distribution of spin label distances with superimposed noise and various test function $\lambda_i(z)$ of the orientation intensity: $\lambda_1(z)=0.25$, $\lambda_2(z)=0.5z$, $\lambda_3(z)=0.5(1-z)$, $\lambda_4(z)=0.5z^2$, $\lambda_5(z)=2(0.5-z)^2$, $\lambda_6(z)=0.5(1-z)^2$, $\lambda_7(z)=0.5(1-z^2)$, $\lambda_8(z)=0.5-2(0.5-z)^2$, and $\lambda_9(z)=0.5[1-(1-z)^2]$. The left panel compares these polynomial functions (black lines) with the regularized orientation intensity functions (red lines) obtained from the deconvolution method. The right panel compares PELDOR time traces as obtained from the input polynomial functions (black lines) and the regularized functions (red lines).

with the input polynomial functions. Moreover, we calculated PELDOR time traces from the regularized orientation intensity functions and compared the results to PELDOR time traces obtained from the polynomial functions. Again, Fig. 2 reveals excellent agreement of regularized and original data. The method was also found to work in cases with broad distance distributions and resulting very weak PELDOR oscillations (data not shown). These findings make us confident to apply the proposed deconvolution method to the analysis of true experimental PELDOR signals.

III. PELDOR STUDY OF NITROXIDE BIRADICALS

A. Experimental details

Recently, dead-time free PELDOR experiments at *X*-band frequencies have been performed on simple nitroxide biradicals.[26] In brief, double-labeled linear and bent biradicals [see Fig. 1(b)] were synthesized and solvated in *ortho*-terphenyl.[12,26,30] The PELDOR measurements were performed in frozen solution at a temperature of 40 K. The duration of the pump pulse was set to $t_B=12$ ns at the resonance frequency of the resonator and the probe pulses length was $t_A=32$ ns. The excitation bandwidth of the pump and probe pulse were chosen small enough to avoid spectral overlap of the pulses even for the lowest detection frequency offset of $\Delta\nu=40$ MHz. On the other hand, the excitation width of the pump pulse should be as large as possible to achieve a deep modulation depth. Figure 3 shows the resulting PELDOR time traces for probe frequencies offsets ranging from 40 to 80 MHz. The signals were normalized to their maximal values at zero time, $T=0$. The intermolecular exponential signal decay is already removed.

B. Determination of the orientation intensity function

The damped oscillations of the PELDOR time traces shown in Fig. 3(a) reveal that the mean distance between the two nitroxide spin labels is ≈3.3 nm for both biradicals [see Eq. (12)]. The somewhat faster damping of the oscillations of compound 2 indicates that the underlying distance distribution is broader for the bent radical 2 as for the linear system 1. Furthermore, the dependence of the oscillation frequency on the offset $\Delta\nu$ indicates the presence of angular correlation effects. Indeed, previous studies[26] have shown that the motion of the spin labels is quite restricted in these molecules. Despite a certain rotational and conformational flexibility, the orientations of the spin labels do not significantly deviate from their minimal energy conformation. This orientation selection can be deduced from the experimental PELDOR time traces by applying the above proposed deconvolution methods to determine the orientation intensity function.

To this end, we employed the following strategy. First, the distance distribution $f(r)$ is estimated by the DEERANALYSIS program described in Ref. 16. In this first step, possible angular correlation effects are disregarded by using the average $S(T)=\Sigma_i S(T,\Delta\nu_i)$ over all offset frequencies $\Delta\nu$ as input data in the Tikhonov regularization. Figure 3(b) shows the resulting spin label distance distribution for compounds 1 and 2. As already anticipated in the discussion of the time traces, the peak of the distribution is located at 3.3 nm for both molecules, while its width is larger for compound 2 than for compound 1. In a second step, the convolution expression (11) is employed to determine the orientation intensity function $\lambda(z)$ from the experimental data via Tikhonov regularization. The resulting functions $\lambda(z)$ obtained for compounds 1 and 2 are displayed in Fig. 3(c). Using these functions in combination with the distance distribution shown in Fig. 3(b), we can recalculate the PELDOR signals. As shown in Fig. 3(a), recalculated and original PELDOR time traces are in absolute agreement, thus demonstrating the internal consistency of the method.

Several technical issues should be mentioned at this point. First, we note that the second step of the procedure [i.e., the evaluation of Eq. (17)] requires to choose the regularization parameter α. Usually, the *L*-curve method[19] is used to determine α. However, it was found that in this case the parametric plot of the deviation of the regularized signal from the experimental data versus the smoothness in loga-

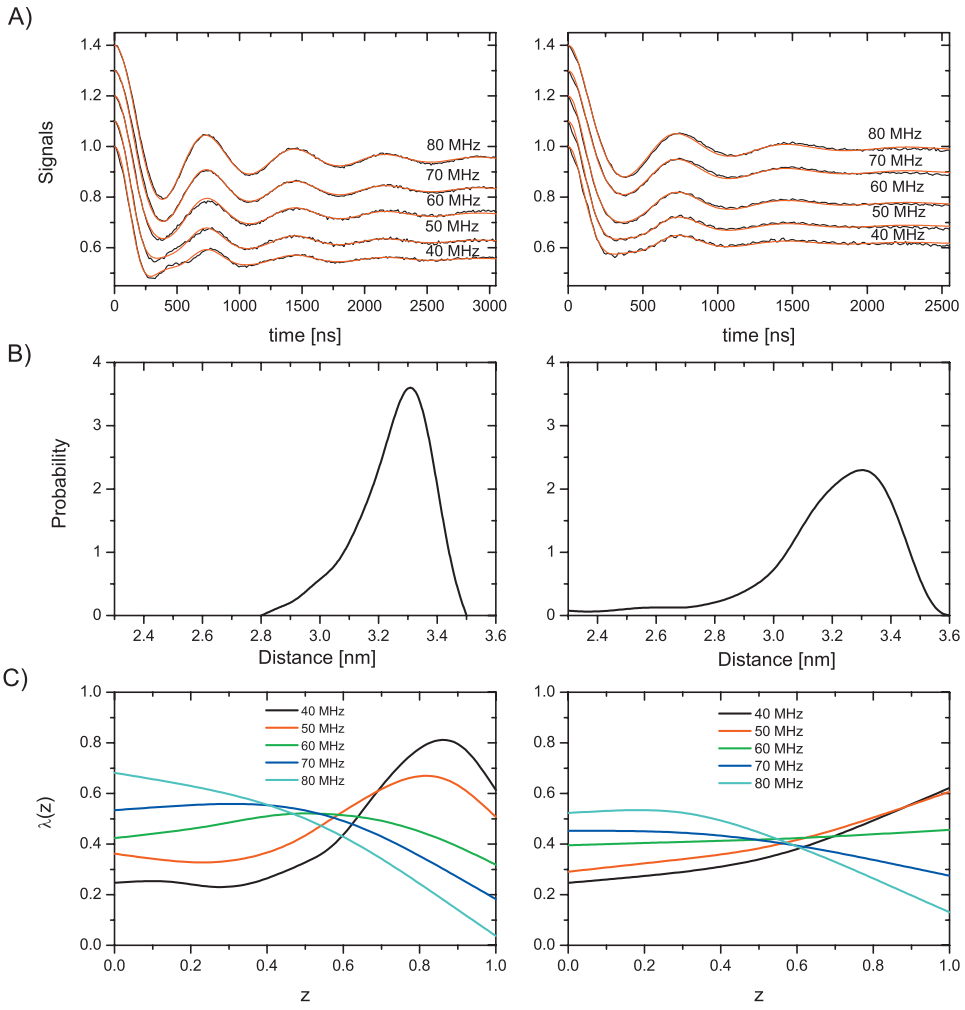

FIG. 3. (Color) Analysis of the PELDOR measurements obtained for compound 1 (left panels) and compound 2 (right panels). (a) Comparison of measured (black lines) and reconstructed (red lines) PELDOR time traces. For convenient presentation, the signals obtained for the offsets 50, 60, 70, and 80 MHz were shifted by 0.1, 0.2, 0.3, and 0.4, respectively. (b) Distribution of the spin label distances, obtained from DEERANALYSIS (Ref. 16) of the averaged time traces (see text). (c) Orientation intensity functions obtained by the Tikhonov regularization, assuming the distance distribution shown in panel (b).

rithmic scale does not yield curves with a pronounced *L*-shape. Therefore, we estimated the regularization parameter by setting a limit ϵ for the deviation between measured and regularized time traces. The parameter ϵ can be estimated from the level of noise and the inaccuracy caused by the elimination of the intermolecular relaxation contribution. For example, if the uniform noise level is 1%, then the logarithm of the averaged squared deviation between experiment and regularized signal is equal to $\epsilon=\log_{10}(1/3\times 0.01^2)=-4.47$. Having determined ϵ, Eq. (17) is solved with the largest overall parameter α. Setting the deviation limit to $\epsilon=-4.47$ we obtain for molecule 1 the regularization parameters $\boldsymbol{\alpha}=3^2$, 3^3, 3^5, 3^7, and 3^7 for the frequency offsets 40, 50, 60, 70, and 80 MHz, respectively. Similarly, we obtain for molecule 2 the values 3^5, 3^5, 3^{10}, 3^8, and 3^8. As the calculation of the regularization parameters is rather approximate, it is reassuring to know that the procedure depends only weakly on the exact choice of α. In all cases considered, the PELDOR time traces are of similar nature, even if the smallest or largest considered value of α is employed.

Furthermore, we note that problems may arise regarding the Tikhonov regularization if the underlying distributions of distance and orientations are not smooth, single-peaked functions but exhibit several, possibly sharp, maxima. This is because the Fredholm integral equation of the first kind (11) is an ill-posed problem, implying that some columns of the kernel matrix $K_{ij}=\langle\cos(D/r^3(1-3z_j^2)T_i)\rangle$ can be nearly linearly dependent, which makes the computed solutions potentially sensitive to small perturbations of the data. For example, we may find that $K_{ij}\approx K_{ij'}$ for all times T_i, even if the corresponding values for z_j and $z_{j'}$ are not similar. (Note that $K(z,T)$ exhibits the same values in the intervals $z\in[0,\sqrt{1/3}]$ and $z\in[\sqrt{1/3},\sqrt{2/3}]$.) Practice has shown so far, however, that orientation intensity functions are usually rather smooth. As a final note of caution we mention that the usual subtraction of intermolecular relaxation from the measured PELDOR time traces may be problematic if the intermolecular decay is nonexponential or in case the PELDOR oscillations exceed the observation time window.

IV. MOLECULAR DYNAMICS STUDY OF NITROXIDE BIRADICALS

A. Simulation details

All molecular dynamics (MD) simulations were performed using the GROMACS (Ref. 31) program package and the AMBER98 (Ref. 32) force field. To specify the potential-energy function of the nitroxide spin label, density functional theory calculations at the B3LYP/6-31+G(*d*) level were performed. All nonstandard force-field parameters (in particular, partial charges, bond lengths, and bond angles) were

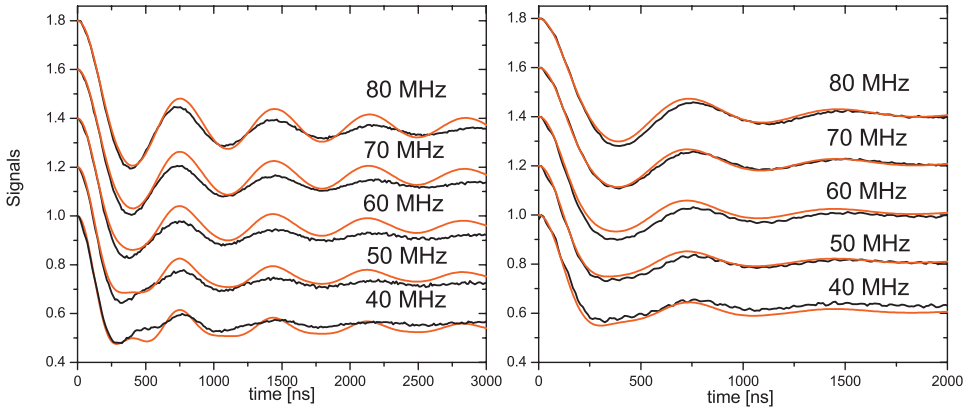

FIG. 4. (Color) Comparison of measured (black lines) and MD simulated (red lines) PELDOR time traces obtained for compound 1 (left) and compound 2 (right).

then derived employing the AMBER strategy of force-field development[33] and published in Ref. 34.

In each simulation, the biradical was solvated in a cubic box of TIP3P water,[35] keeping a minimum distance of 10 Å between the solute and each face of the box. The simulation system contained 13 999 atoms in a box of the dimension $53\times53\times53$ Å^3. The equation of motion was integrated by using a leap frog algorithm with a time step of 2 fs. Covalent bond lengths involving hydrogen atoms were constrained by the LINC algorithm[36] with a relative geometric tolerance of 0.0001. A cutoff of 10 Å was used for the nonbonded van der Waals interactions, and the nonbonded interaction pair list was updated every 10 fs. Periodic boundary conditions were applied and the particle mesh Ewald method[37] was used to treat electrostatic interactions. The solute and solvent were separately weakly coupled to external temperature baths at 250 or 350 K with a temperature coupling constant of 0.5 ps (0.01 during the first 100 ps). The whole system was first minimized for 1000 steps, then a 100 ps MD run was performed. The simulation was then continued for 20 ns, where the coordinates were saved every picosecond for analysis.

For the resulting ensemble of 20 000 conformational structures, we calculated the PELDOR time traces as described in Sec. II A. We employed the magnetic parameters $g_{xx}=2.0088$, $g_{yy}=2.007$, and $g_{zz}=2.0025$, as well as $A_{xx}=5$ G, $A_{yy}=5$ G, and $A_{zz}=33$ G. The strength of the external magnetic field was set to 3450 G, which corresponds to a pump-pulse frequency of 9.721 GHz. The value of the inhomogeneous line width was taken equal to 6 G.

B. Calculation of PELDOR signals

The resulting simulated PELDOR time traces for both molecular systems are shown in Fig. 4. Considering the fact that parameters were not adjusted, the overall agreement between theory and experiment is remarkable. In the case of the bent system 2, the MD results match the experimental signals almost quantitatively. In the case of the linear system 1, the frequency of the oscillations is reproduced faithfully, while the simulations somewhat underestimate the overall damping of the experimental signal. The latter finding already indicates that the width of the interspin distance distribution is somewhat too small in the MD description of system 1. Indeed, the comparison of distance distributions extracted from experimental time traces and from MD simulations in Fig. 5 reconfirms this finding and also shows that both mean values and the distance distribution of system 2 are reproduced very well. Figure 5 also shows a comparison for the orientation intensity functions from both methods. Again, we find almost quantitative agreement in the case of the bent system 2. The calculated intensity functions of the

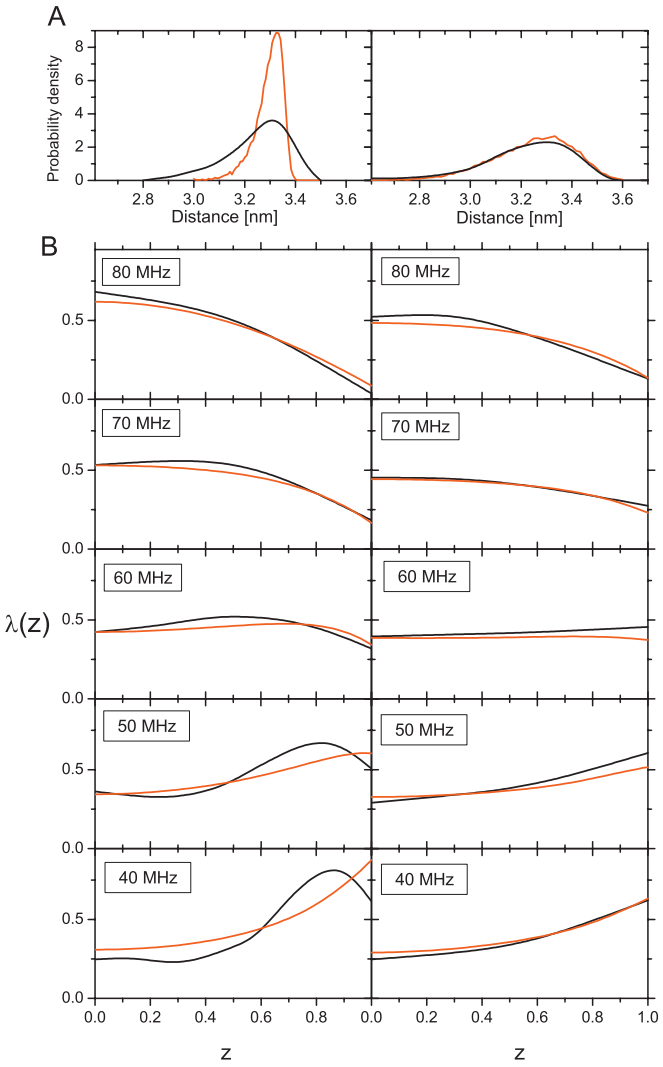

FIG. 5. (Color) (a) Distributions of spin label distances and (b) orientational intensity functions as obtained for the linear biradical (left panels) and bent biradical (right panels). Compared are experimental results from a Tikhonov regularization (black lines) and calculated results from a MD simulation (red lines).

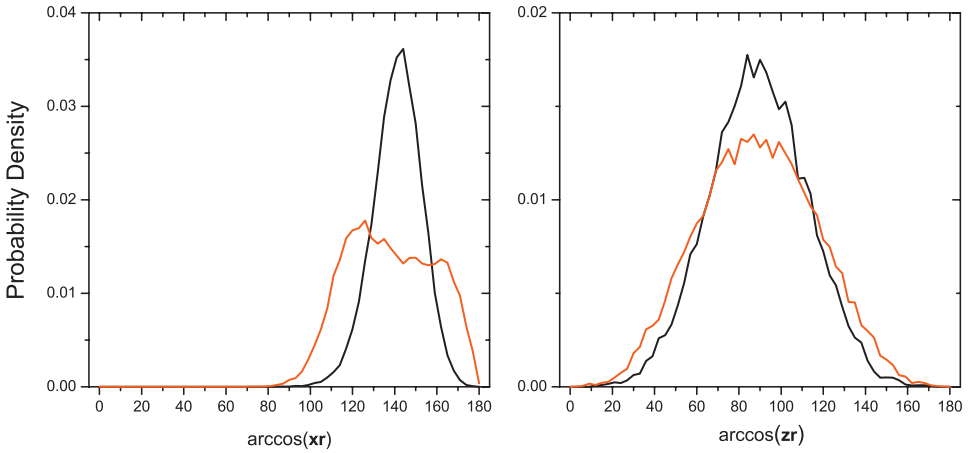

FIG. 6. (Color) MD simulation results for the orientation distribution of the spin labels in the linear (black lines) and bent (red lines) biradical. Shown are the distributions of (left) the angle between the dipolar vector $\boldsymbol{r}$ and the normal of the radical plane z_i and (right) the angle between $\boldsymbol{r}$ and the NO axis of the spin label.

linear system 1, on the other hand, agree only well with experiment at high frequency offsets (60–80 MHz), but deteriorate at low offsets (40–50 MHz). Assuming that the proposed Tikhonov regularization procedure works well for this simple example, the deviations between theory and experiment are most likely caused by inaccuracies of the empirical force field. Furthermore, it should be kept in mind that we have initially assumed that the thermal distribution of conformational states (as seen in MD simulations) is preserved in a PELDOR experiment using a frozen sample.[26]

Having validated the MD simulations by comparison to the experiment, we are now in a position to investigate the orientational distribution of the spin labels as predicted by the simulations. To this end, we first considered the angle $\varphi \equiv \arccos(z_1 \cdot z_2)$ describing the relative orientation of the two labels. As may be expected, we find that the angle φ is uniformly distributed, which reflects the almost free rotation of the nitroxides around their connecting bond axes. Next we considered two angles describing the relative orientation of the labels and the dipolar vector $\boldsymbol{r}$, that is, $\beta_i \equiv \arccos(z_i \cdot \boldsymbol{r})$ and $\delta_i \equiv \arccos(\boldsymbol{x}_i \cdot \boldsymbol{r})$ with $i=1,2$, see Fig. 1. The distributions of these angles are shown in Fig. 6. For both molecular systems, we see that $\beta_i = 90° \pm 30°$, i.e., on average the normal of the radical plane, z_i, is perpendicular to the connecting dipolar vector $\boldsymbol{r}$. The angle δ_i between the NO axis of the label and the dipolar vector, on the other hand, exhibits a mean value of $\approx 140°$ for 1. As expected from their molecular structures, the bent system 2 shows a larger fluctuations of the angle δ_i than the molecule 1, due to the free rotation of the nitroxides.

V. DISCUSSION AND CONCLUSIONS

Ansatz (11) for the PELDOR signals allows us to obtain both distance information [i.e., the distribution $f(r)$] and orientational information [i.e., the function $\lambda(\cos \Theta)$] from a PELDOR experiment. Adopting various polynomials as orientation intensity functions, we have shown the internal consistency of this approach, that is, recalculated and original PELDOR time traces are in good agreement (Fig. 3). Furthermore, we have shown that PELDOR signals, distance distributions, and orientational intensity functions obtained from the experimental data of small nitroxide biradicals and from MD simulations agree quite well (Figs. 4 and 5). The differences between the results obtained by both methods are surprisingly small, taking into account that the MD studies are performed in liquid water solution at room temperature, whereas PELDOR experiments were performed in frozen solution samples in *ortho*-terphenyl at 40 K. The observed differences might also be due to the limitations of both methods. On one hand, the precision of the Tikhonov regularization can be enhanced by an improved choice of the regularization parameter. On the other hand, MD simulation results can be improved by a more accurate determination of empirical force fields.

An analysis of the MD trajectories has revealed that (i) the spin labels rotate freely around their connecting bond axes, (ii) the normal of the radical planes is on average perpendicular to the connecting dipolar vector, and (iii) the angle between the NO axis of the labels and the dipolar vector is on average $\approx 140°$ for compound 1 whereas it is more or less uniformly distributed in the interval (110°,170°) for the compound 2 (Fig. 6). At this point, the question arises to what extent this orientational information can also be inferred directly from the PELDOR experiments, i.e., by analysis of the orientational intensity functions $\lambda(\cos \Theta)$. Generally speaking, all curves $\lambda(\cos \Theta)$ as shown in Fig. 5(b) are relatively flat for $0 \leq \cos \Theta \leq 0.5$, although their levels are gradually increased for larger frequency offsets $\Delta\nu$. That is, all molecules are similarly excited for small values of $\cos \Theta$, i.e., for angles $\Theta \equiv \arccos(\boldsymbol{r} \cdot \boldsymbol{B}_0) \approx 90°$ $(\boldsymbol{r} \perp \boldsymbol{B}_0)$. For large values of $\cos \Theta$ corresponding to $\Theta \approx 0°$ $(\boldsymbol{r} \| \boldsymbol{B}_0)$, we observe a strong intensity at small frequency offsets and a weak intensity at large offset frequencies. To relate this finding to the underlying structure of the molecules, we recall that for small frequency offsets we preferentially have $z_i \perp \boldsymbol{B}_0$. Assuming that $z_i \perp \boldsymbol{r}$, biradicals with both $\boldsymbol{r} \perp \boldsymbol{B}_0$ and $\boldsymbol{r} \| \boldsymbol{B}_0$ can be excited, i.e., λ has nonzero values for all $0 \leq \cos \Theta \leq 1$. For large frequency offsets, on the other hand, we find $z_i \| \boldsymbol{B}_0$. In this case, only biradicals with $\boldsymbol{r} \perp \boldsymbol{B}_0$ can be excited, i.e., λ vanishes for $\cos \Theta \approx 1$. In particular, for molecule 1 these structural constraints can be predicted from the orientational function $\lambda(\cos \Theta)$.

To summarize, we have shown that it is possible to separate the distance distribution function $f(r)$ from an intensity function $\lambda(\cos \Theta)$ which only contains orientational information. The latter function has a clear physical meaning, as it

reflects the PELDOR intensities from molecules with different orientations in the external magnetic field. Dependence of function λ on the probe pulse frequency offset $\Delta\nu$ can be considered as a spectrum, which is determined by the orientations of the spin labels and vector ***r***. The orientation intensity function is directly obtained from the experimental data and its calculation is easier than the calculation of PELDOR time traces based on MD trajectories. Therefore, the function λ can be conveniently used for the comparison of MD studies with experiments. In the present work we compared the intensity function obtained from PELDOR experiments by Tikhonov regularization with intensity function calculated from MD simulations for two model dinitroxide compounds and achieved excellent agreement in both cases. The orientational information does not only yield the structure of the molecule but is also essential for a quantitative analysis of the molecular dynamics encoded in the attenuation of the PELDOR signal. Applications of this approach to biological macromolecules and a quantitative determination of the polar angle of the dipolar vector ***r*** in the nitroxide molecular axis system using probe pulse frequency dependence of the function λ are currently in progress.

ACKNOWLEDGMENTS

We thank Olav Schiemann and Bela E. Bode for numerous inspiring and helpful discussions. This work has been supported by the Deutsche Forschungsgemeinschaft (via Grant No. SFB 579), the Center of Biomolecular Magnetic Resonance and by the Frankfurt Center for Scientific Computing. Y.M. gratefully acknowledges the URC (Grant No. RG65/06) from the Nanyang Technological University and Academic Research Fund (AcRF) Tier 2 (Grant No. T206B3210RS) by the MOE. D.M. is grateful for a Center of Membrane Proteomics fellowship.

[1] A. D. Milov, K. M. Salikhov, and J. E. Shirov, Fiz. Tverd. Tela (Leningrad) **23**, 975 (1981).
[2] A. D. Milov, A. B. Ponomarev, and Y. D. Tsvetkov, J. Chem. Phys. **60**, 4508 (1984).
[3] J. H. Freed, Annu. Rev. Phys. Chem. **51**, 655 (2000).
[4] P. Borbat and J. Freed, Methods Enzymol. **423**, (C), 52 (2007).
[5] A. Schweiger and G. Jeschke, *Principles of Pulsed Electron Paramagnetic Resonance* (Oxford University Press, Oxford, 2001).
[6] O. Schiemann and T. Prisner, Q. Rev. Biophys. **40**, 1 (2007).
[7] Y. D. Tsvetkov, A. D. Milov, and A. G. Maryasov, Russ. Chem. Rev. **77**, 487 (2008).
[8] J. R. Lakowicz, *Principles of Fluorescence Spectroscopy* (Plenum, New York, 1999).
[9] R. S. Keyes and A. M. Bobst, Biochemistry **34**, 9265 (1995).
[10] O. Schiemann, N. Piton, Y. Mu, G. Stock, J. Engels, and T. F. Prisner, J. Am. Chem. Soc. **126**, 5722 (2004).
[11] N. Piton, Y. Mu, G. Stock, T. Prisner, O. Schiemann, and J. Engels, Nucleic Acids Res. **35**, 3128 (2007).
[12] O. Schiemann, N. Piton, J. Plackmeyer, B. Bode, T. Prisner, and J. Engels, Nat. Protocols **2**, 904 (2007).
[13] Q. Cai, A. K. Kusnetzow, W. L. Hubell, I. S. Haworth, G. P. C. Gacho, N. Eps, K. Hideg, E. J. Chambers, and P. Z. Qin, Nucleic Acids Res. **34**, 4722 (2006).
[14] M. Chen, M. Margittai, J. Chen, and R. Langen, J. Biol. Chem. **282**, 24970 (2007).
[15] G. Sicoli, G. Mathis, O. Delalande, Y. Boulard, D. Gasparutto, and S. Gambarelli, Angew. Chem., Int. Ed. **47**, 735 (2008).
[16] G. Jeschke, G. Panek, A. Godt, A. Bender, and H. Paulsen, Appl. Magn. Reson. **26**, 223 (2004).
[17] G. Jeschke, A. Bender, H. Paulsen, H. Zimmermann, and A. Godt, J. Magn. Reson. **169**, 1 (2004).
[18] G. Jeschke and Y. Polyhach, Phys. Chem. Chem. Phys. **9**, 1895 (2007).
[19] Y. Chiang, P. Borbat, and J. Freed, J. Magn. Reson. **172**, 279 (2005).
[20] Y. Chiang, P. Borbat, and J. Freed, J. Magn. Reson. **177**, 184 (2005).
[21] V. Denysenkov, T. F. Prisner, J. Stubbe, and M. Bennati, Proc. Natl. Acad. Sci. U.S.A. **103**, 13386 (2006).
[22] V. Denysenkov, D. Biglino, W. Lubitz, T. Prisner, and M. Bennati, Angew. Chem., Int. Ed. **47**, 1224 (2008).
[23] R. G. Larsen and D. J. Singel, J. Chem. Phys. **98**, 5134 (1993).
[24] A. D. Milov, A. G. Maryasov, and Y. D. Tsvetkov, Appl. Magn. Reson. **15**, 107 (1998).
[25] A. G. Maryasov, Y. D. Tsvetkov, and J. Raap, Appl. Magn. Reson. **14**, 101 (1998).
[26] D. Margraf, B. Bode, A. Marko, O. Schiemann, and T. Prisner, Mol. Phys. **105**, 2153 (2007).
[27] M. Pannier, S. Viet, A. Godt, G. Jeschke, and H. W. Spiess, J. Magn. Reson. **142**, 331 (2000).
[28] Y. Polyhach, A. Godt, C. Bauer, and G. Jeschke, J. Magn. Reson. **185**, 118 (2007).
[29] A. Marko, B. Wolter, and W. Arnold, J. Magn. Reson. **185**, 19 (2007).
[30] B. Bode, D. Margraf, J. Plackmeyer, G. Dürner, T. Prisner, and O. Schiemann, J. Am. Chem. Soc. **129**, 6736 (2007).
[31] E. Lindahl, B. Hess, and D. van der Spoel, J. Mol. Model. **7**, 306 (2001).
[32] T. E. Cheatham, P. Cieplak, and P. A. Kollman, J. Biomol. Struct. Dyn. **16**, 845 (1999).
[33] D. Case, D. Pearlman, J. Caldwell, T. C. III, J. Wang, W. Ross, C. Simmerling, T. Darden, R. Stanton, A. Cheng *et al.*, AMBER 7, University of California, San Francisco, CA, 1999.
[34] H. Yu, Y. Mu, L. Nordenskiold, and G. Stock, J. Chem. Theory Comput. **4**, 1781 (2008).
[35] W. L. Jorgensen, J. Chandrasekhar, J. D. Madura, R. W. Impey, and M. Klein, J. Chem. Phys. **79**, 926 (1983).
[36] B. Hess, H. Bekker, H. J. C. Berendsen, and J. G. E. M. Fraaije, J. Comput. Chem. **18**, 1463 (1997).
[37] T. Darden, D. York, and L. Petersen, J. Chem. Phys. **98**, 10089 (1993).